Anti-CD4-targeted Gold Nanoparticles Induce Specific Contrast Enhancement of Peripheral Lymph Nodes in X-ray Computed Tomography of Live Mice

ARTICLE *in* NANO LETTERS · MAY 2010

Impact Factor: 13.59 · DOI: 10.1021/nl101019s · Source: PubMed

NANO LETTERS

pubs.acs.org/NanoLett

Anti-CD4-targeted Gold Nanoparticles Induce Specific Contrast Enhancement of Peripheral Lymph Nodes in X-ray Computed Tomography of Live Mice

Wolfgang Eck,*,[⊥] Anthony I. Nicholson,[§] Hanswalter Zentgraf,[†] Wolfhard Semmler,[||] and Sönke Bartling[||]

[⊥]Applied Physical Chemistry, University of Heidelberg, Im Neuenheimer Feld 253, Heidelberg, Germany, [§]The Jackson Laboratory, Technology Evaluation and Development, Physiology & in vivo Imaging, Bar Harbor, Maine, U.S.A., [†]German Cancer Research Center, Department of Tumor Virology, Heidelberg, Germany, and [||]German Cancer Research Center, Department of Medical Physics in Radiology, Heidelberg, Germany

ABSTRACT Antibody-conjugated gold nanoparticles have been applied as a biologically targeted contrast agent in live mice for one of the most widely used medical imaging methods, X-ray computed tomography. Such nanoprobes directed toward the CD4 receptor lead to distinctly enhanced X-ray contrast of peripheral lymph nodes. This study demonstrates the general feasibility of biologically specific X-ray imaging in living animals and discusses basic requirements for the use of nanoparticles as a targeted X-ray contrast agent.

KEYWORDS anti-CD4 antibodies, biologically targeted in vivo imaging, contrast agent, gold nanoparticles, X-ray computed tomography

X-ray computed tomography (X-ray CT) is a widely utilized imaging procedure in medicine. In today's clinical practice, polyiodinated aromatic molecules are routinely used for contrast enhancement.[1−4] Rapid renal excretion of these agents is ensured due to their low molecular weight, and imaging with enhanced contrast is possible within a time frame of seconds up to a few minutes. Commonly, X-ray CT is not being considered as a suitable method for biologically targeted imaging, because it is less sensitive in detecting targeted agents compared to other imaging methods, such as positron emission tomography (PET) or magnetic resonance imaging (MRI).[5,6] Targeted imaging of distinct cell or tissue types in X-ray CT requires that large volumes of heavy elements with high X-ray absorption are selectively delivered to a biologically defined site. However, such targeted contrast agents with sufficient X-ray absorption have not yet been developed for application in vivo.[7,8] Nanoparticles conjugated to biological directing agents such as peptides or antibodies can be suitable for such purposes, as they can transport a large amount of a heavy element to a single biological receptor. In this communication, we show that gold nanoparticles conjugated to anti-CD4 monoclonal antibodies provide molecularly selective contrast enhancement of peripheral lymph nodes in living mice that can be detected by X-ray computed tomography.

Recently, the suitability of gold[9−14] and bismuth sulfide[15] nanoparticles as nontargeted X-ray contrast agents has been demonstrated in live mice. Bismuth sulfate and barium sulfate filled microcapsules have been used for X-ray-guided delivery and imaging of cellular therapeutics.[16] Iodinated nanoparticles have been examined as X-ray contrast agents in several other studies.[17−27] In a first attempt to use antibody-conjugated gold nanoparticles as a biologically targeted contrast agent for X-ray CT, their binding to cancer cells in culture has been investigated.[28] Biologically targeted magnetic nanoparticles as contrast agents for magnetic resonance imaging (MRI) in living animals have been investigated in several studies.[29−38]

In order to prepare nanoparticles suitable for application in living organisms, their surface is often covered with biocompatible polymers such as polyethylene glycol (PEG) or polyvinylpyrrolidone (PVP) that stabilize the particles in the bloodstream.[39,40] These surface coatings inhibit rapid uptake of the particles by scavenger cells such as macrophages and lead to prolonged circulation times (the "blood-pool effect"). Such nanoparticles have also been termed "stealth particles". Generally, non-biologically degradable nanoparticles with a diameter larger than about 5 nm are not renally excreted,[41] and thus nanoparticles with higher diameters permit significantly longer imaging times than do standard low-molecular weight contrast agents.

In a recent study, we have prepared gold nanoparticles coated with heterobifunctional polyethylene glycol (h-PEG) that were conjugated to monoclonal antibodies (mAb F19)

* To whom correspondence should be addressed. E-mail: w-eck@uni-hd.de.
Received for review: 09/19/2009
Published on Web: 00/00/0000

DOI: 10.1021/nl101019s | *Nano Lett.* **XXXX,** *xxx,* 000–000

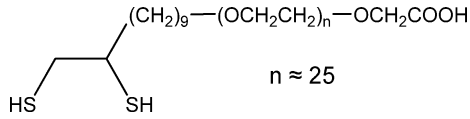

FIGURE 1. Heterobifunctional PEG ligand used to stabilize the gold nanoparticles. The molecules bear a dithiol group as an anchor group to the gold surface and a carboxy group for covalent attachment of antibodies to the outside of the ligand shell.

as a targeting moiety.[42] IgG antibodies show full retention of their biological selectivity when they are attached to the outside of a protein-repellent PEG shell, as opposed to similar surfaces not stabilized by a biocompatible polymer.[43] Such mAb F19 conjugated nanoparticles directed against fibroblast activation protein (FAP-α) selectively stained the tumor stroma of human pancreatic cancer tissue resected from patients[42] and could be visualized by scattered light using a simple optical microscope setup.

A major challenge in targeted X-ray imaging of biological systems is the realization of a high local concentration of the contrast agent that is large enough to surpass the X-ray absorption of oxygen and carbon, the two major background components. The targeted contrast agent should bind to a receptor with a sufficiently high concentration in the selected tissue. For our first experiments, we chose the CD4 receptor, which has a high occurrence on T cells and macrophages, and has been reported to reach concentrations of approximately 32000 molecules per cell on peripheral blood mononuclear T cells of HIV negative humans.[44] In mammals, T cells and CD4 receptors are found in particularly high concentration in lymph nodes and the spleen.

As the contrast agent, we prepared gold nanoparticles stabilized by a heterobifunctional PEG ligand (Figure 1). This ligand bears a dithiol anchor group on one end of the PEG chain and a terminal carboxy group for coupling of antibody molecules on the other end, and can be easily attached to citrate-stabilized gold nanoparticles by ligand exchange in water.[42] Anti-mouse CD4 (clone GK1.5) monoclonal antibodies were coupled to the PEG stabilized particles using a procedure based on *N*-hydroxysuccinimide/1-ethyl-3-(3-dimethylaminopropyl) carbodiimide (NHS/EDC), similar to the method described in ref 42. The particle−antibody conjugates were characterized using transmission electron microscopy after drying of dilute samples on commercially available copper grids bearing a 20-nm thick carbon film.

Two different sizes of individual gold nanoparticles were used, with average diameters of the single gold particles of 28 ± 7 nm and 38 ± 8 nm (Figure 2). These values were determined by transmission electron microscopy (TEM) by measuring Feret's diameter of at least 50 different particles in each sample. (Feret's diameter is the longest measurable

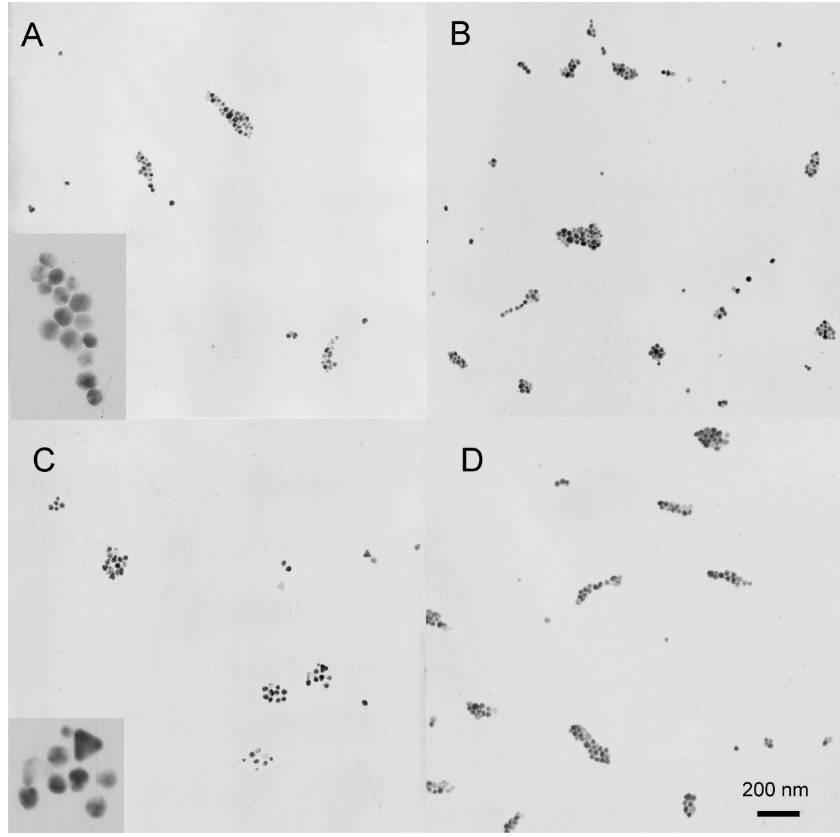

FIGURE 2. TEM images of PEGylated gold nanoparticles conjugated to anti-CD4 IgG (A, C) and to nonspecific IgG (B, D). Average Feret diameters of single gold particles are 28 ± 7 nm in A and B, and 38 ± 8 nm in C and D. Larger particle aggregates are visible in all samples. The insets in A and C show individual particle clusters at higher magnification (width of the insets =150 nm).

DOI: 10.1021/nl101019s | *Nano Lett.* **XXXX,** *xxx,* 000–000

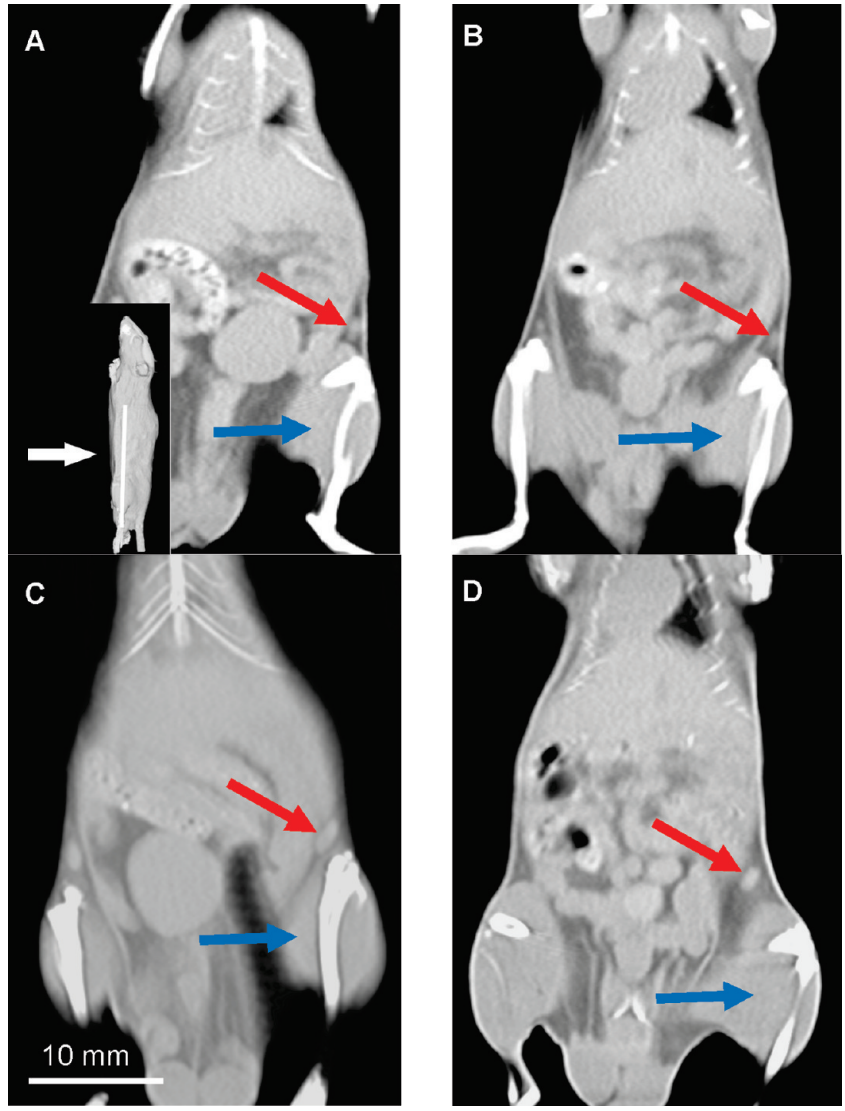

FIGURE 3. X-ray CT images of mice before (A, B) and 1 h after (C, D) injection of gold nanoparticles (38 nm individual diameter) conjugated to unspecific IgG (C) and anti-CD4 IgG (D). The inlay in A provides orientation of the reformatted plane of the abdomen of the mice, where the arrow points along the viewing direction. The targeted (anti-CD4 IgG) nanoparticles show clear contrast enhancement of inguinal lymph nodes (red arrows in B and D), whereas virtually no change is visible for the nonspecific controls (red arrows in A and C). For better visual comparability of X-ray densities, the hind limb muscles have been labeled and set to a standard brightness value (blue arrows). Average measured X-ray densities of the individual lymph nodes (red arrows) in Hounsfield units (HU) are 47 HU (A), 26 HU (B), 52 HU (C), 121 HU (D).

distance between any two points along the boundary of a particle with irregular shape.) After antibody coupling, all samples showed the presence of particle aggregates with maximum extensions of up to ~500 nm (Figure 2). These aggregates, as has been described by Eck et al.,[42] are formed by covalent cross-linking of the carboxy-functionalized nanoparticles by amino groups on the antibody, and potentially by agglomeration during centrifugation. When the samples for TEM imaging were prepared from highly dilute solutions, aggregates were still visible. We can therefore largely rule out that aggregates are formed during drying on the TEM grids. The presence of larger particle aggregates may be beneficial for successful targeted X-ray labeling of the CD4 receptor. When such aggregates are bound to a single receptor molecule, the total amount of gold in the target tissue may become sufficiently large that the X-ray absorption by gold may surpass the normally dominating background X-ray absorption by carbon and oxygen.

For the X-ray CT experiments, 200 μL of a dispersion of gold nanoparticle−anti-mouse CD4 conjugates in standard PBS buffer were injected into the tail vein of living mice (strain C57BL/6, 3 mice per gold nanoparticle size) using a gold concentration of 7 mg per mL, so that the total amount of gold injected per mouse was 1.4 mg. As a negative control, gold nanoparticles of the same diameters coupled to nonspecific monoclonal IgG2b isotype control antibodies were used in 6 other mice. Imaging of the animals was performed before injection and after 1 and 48 h on a flat-

DOI: 10.1021/nl101019s | *Nano Lett.* **XXXX,** *xxx,* 000–000

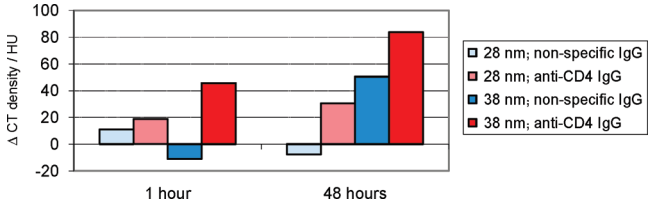

FIGURE 4. Average CT density differences (HU = Hounsfield units) of inguinal lymph nodes between the baseline scan before injection, and 1 or 48 h after injection of gold nanoparticles, respectively. Four different nanoparticle samples (28 nm; control IgG2b isotype IgG; 28 nm; anti-CD4 IgG; 38 nm; control IgG; 38 nm; anti-CD4 IgG) were injected in the tail vein of living mice. Three different mice were used for each sample. Anti-CD4-targeted nanoparticles induced higher contrast enhancement than control particles of identical size in all cases, and larger particles led to stronger enhancement than smaller particles.

panel-based micro X-ray CT[45] using a tube current of 50 mA, a tube voltage of 80 kV, and a scan time of 20 s. A water phantom placed next to the hip of the animals was used to normalize X-ray absorption. Contrast enhancement of inguinal lymph nodes could be detected by X-ray CT in all animals treated with the anti-CD4-targeted nanoparticles. The enhancement caused by the targeted nanoparticles was in all cases higher than the enhancement by the nonspecific control samples of the same size, and the contrast enhancement by larger particles was stronger than by smaller particles (Figures 3 and 4).

Additional mice treated with the larger particles were sacrificed after 5 days, the inguinal lymph nodes resected, fixed with glutaraldehyde and osmium tetroxide, dehydrated, embedded and processed for ultrathin sectioning. TEM images of these samples show a significant excess of gold nanoparticles in the lymph node tissue of animals treated with anti-CD4 conjugated nanoparticles compared to mice treated with the nonspecific control nanoparticles (Figure 5).

Since macrophages, T cells and other scavenger cells all contain the CD4 receptor, we assume as a likely mechanism of nanoparticle enrichment that such cells selectively collect anti-CD4 conjugated gold nanoparticles over a period of several hours, transport them to lymph nodes and increase the local X-ray density. The control nanoparticles not actively targeted to scavenger cells accumulated more weakly in peripheral lymph nodes in all cases. After a period of 48 h, the larger control particles showed some noticeable contrast enhancement as well (Figure 4), probably due to nonspecific uptake by macrophages occurring on a slower time scale. For all particles, liver and spleen started to enhance after this time which corresponds to their well described clearing function of particulate substances.

In essence, this may be regarded as a presentation of biologically targeted X-ray CT imaging by nanoparticles in a living organism. Alternatively, since macrophages and other scavenger cells containing the CD4 antigen generally cause nonselective clearance of all kinds of particles from the bloodstream[27,46] and slow transport to lymph nodes, the

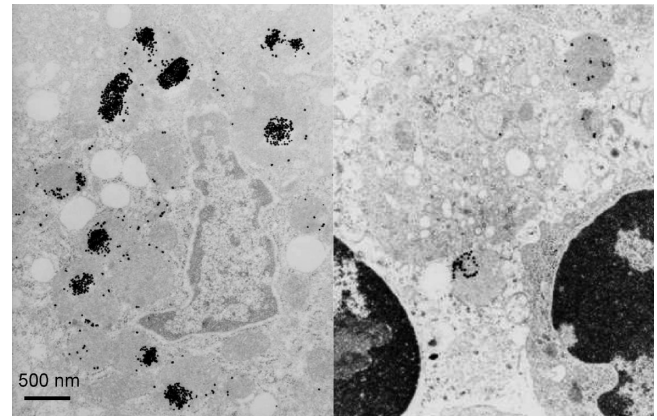

FIGURE 5. Representative TEM images of ultrathin sections of resected inguinal lymph node tissue after fixation with glutaraldehyde and osmium tetroxide. Left: resected from an animal treated with gold nanoparticles (38 nm) conjugated to anti-CD4 IgG. Right: resected from an animal treated with nanoparticles of the same size conjugated to IgG2b isotype control antibodies. The large dark areas in the right image are cell nuclei strongly stained by osmium tetroxide.

effects observed may be described as nanoparticle accumulation in lymph nodes selectively amplified by anti-CD4 targeting. In this respect, we emphasize that many tumors or inflamed tissues also accumulate targeted as well as nontargeted nanoparticles nonselectively due to enhanced permeability and retention (EPR),[39,47–51] which may be increased or accelerated by biological targeting. For disease-related targeting, it will be important to determine exact differences in uptake kinetics and biodistribution between targeted and control nanoparticles. Generally, for targeted X-ray imaging in vivo, a multitude of fundamental questions remain, for example how contrast enhancement by biologically targeted nanoparticles could be achieved in tissues with lower antigen concentrations or different uptake mechanisms.

Acknowledgment. We thank Ted Duffy, Rob Wilpan, and Mike Mason for helpful and stimulating discussions, Marc Brockmann and Sebastian Schambach for their assistance in CT experiments, and we appreciate Michael Grunze's and Barbara Knowles's general support. This work was supported in part by the National Science Foundation/EPSCoR under Grant No. 0132384.

Supporting Information Available. Experimental details of the preparation of gold nanoparticle–antibody conjugates and of X-ray computed tomography. This material is available free of charge via the Internet at http://pubs.acs.org.

REFERENCES AND NOTES

(1) Rutten, A.; Prokop, M. *Anti-Cancer Agents Med. Chem.* **2007**, *7* (3), 307–316.
(2) Christiansen, C. *Toxicology* **2005**, *209* (2), 185–187.
(3) Idee, J.-M.; Nachman, I.; Port, M.; Petta, M.; Le Lem, G.; Le Greneur, S.; Dencausse, A.; Meyer, D.; Corot, C. *Top. Curr. Chem.* **2002**, *222*, 151–171.
(4) Krause, W.; Schneider, P. W. *Top. Curr. Chem.* **2002**, *222*, 107–150.

DOI: 10.1021/nl101019s | *Nano Lett.* **XXXX,** *xxx,* 000–000

(5) Cai, W.; Chen, X. *Small* **2007**, *3* (11), 1840–1854.
(6) Pan, D.; Lanza, G. M.; Wickline, S. A.; Caruthers, S. D. *Eur. J. Radiol.* **2009**, *70* (2), 274–285.
(7) Speck, U. *Handb. Exp. Pharmacol.* **2008**, *185* (Pt. 1), 167–175.
(8) Debbage, P.; Jaschke, W. *Histochem. Cell Biol.* **2008**, *130* (5), 845–75.
(9) Hainfeld, J. F.; Slatkin, D. N.; Focella, T. M.; Smilowitz, H. M. *Br. J. Radiol.* **2006**, *79* (939), 248–253.
(10) Cai, Q.-Y.; Kim, S. H.; Choi, K. S.; Kim, S. Y.; Byun, S. J.; Kim, K. W.; Park, S. H.; Juhng, S. K.; Yoon, K.-H. *Invest. Radiol.* **2007**, *42* (12), 797–806.
(11) Kim, D.; Park, S.; Lee, J. H.; Jeong, Y. Y.; Jon, S. *J. Am. Chem. Soc.* **2007**, *129* (24), 7661–7665.
(12) Kattumuri, V.; Katti, K.; Bhaskaran, S.; Boote, E. J.; Casteel, S. W.; Fent, G. M.; Robertson, D. J.; Chandrasekhar, M.; Kannan, R.; Katti, K. V. *Small* **2007**, *3* (2), 333–341.
(13) Alric, C.; Taleb, J.; Le Duc, G.; Mandon, C.; Billotey, C.; Le Meur-Herland, A.; Brochard, T.; Vocanson, F.; Janier, M.; Perriat, P.; Roux, S.; Tillement, O. *J. Am. Chem. Soc.* **2008**, *130* (18), 5908–5915.
(14) Hall, C. J.; Schultke, E.; Rigon, L.; Ataelmannan, K.; Rigley, S.; Menk, R.; Arfelli, F.; Tromba, G.; Pearson, S.; Wilkinson, S.; Round, A.; Crittell, S.; Griebel, R.; Juurlink, B. H. J. *Eur. J. Radiol.* **2008**, *68* (3 Suppl.), S156–S159.
(15) Rabin, O.; Manuel Perez, J.; Grimm, J.; Wojtkiewicz, G.; Weissleder, R. *Nat. Mater.* **2006**, *5* (2), 118–122.
(16) Barnett, B. P.; Kraitchman, D. L.; Lauzon, C.; Magee, C. A.; Walczak, P.; Gilson, W. D.; Arepally, A.; Bulte, J. W. M. *Mol. Pharmaceutics* **2006**, *3* (5), 531–538.
(17) Aviv, H.; Bartling, S.; Kieslling, F.; Margel, S. *Biomaterials* **2009**, *30* (29), 5610–5616.
(18) Karathanasis, E.; Suryanarayanan, S.; Balusu Sri, R.; McNeeley, K.; Sechopoulos, I.; Karellas, A.; Annapragada Ananth, V.; Bellamkonda Ravi, V. *Radiology* **2009**, *250* (2), 398–406.
(19) Ashcroft, J. M.; Hartman, K. B.; Kissell, K. R.; Mackeyev, Y.; Pheasant, S.; Young, S.; Van der Heide, P. A. W.; Mikos, A. G.; Wilson, L. J. *Adv. Mater.* **2007**, *19* (4), 573–576.
(20) Galperin, A.; Margel, D.; Baniel, J.; Dank, G.; Biton, H.; Margel, S. *Biomaterials* **2007**, *28* (30), 4461–4468.
(21) Galperin, A.; Margel, D.; Margel, S. *J. Biomed. Mater. Res., Part A* **2006**, *79A* (3), 544–551.
(22) Galperin, A.; Margel, S. *Biomacromolecules* **2006**, *7* (9), 2650–2660.
(23) Galperin, A.; Margel, S. *J. Polym. Sci., Part A: Polym. Chem.* **2006**, *44* (12), 3859–3868.
(24) Galperin, A.; Margel, S. *J. Biomed. Mater. Res., Part B* **2007**, *83B* (2), 490–498.
(25) Hyafil, F.; Cornily, J.-C.; Feig, J. E.; Gordon, R.; Vucic, E.; Amirbekian, V.; Fisher, E. A.; Fuster, V.; Feldman, L. J.; Fayad, Z. A. *Nat. Med.* **2007**, *13* (5), 636–641.
(26) Kong, W. H.; Lee, W. J.; Cui, Z. Y.; Bae, K. H.; Park, T. G.; Kim, J. H.; Park, K.; Seo, S. W. *Biomaterials* **2007**, *28* (36), 5555–5561.
(27) McIntire, G. L.; Bacon, E. R.; Illig, K. J.; Coffey, S. B.; Singh, B.; Bessin, G.; Shore, M. T.; Wolf, G. L. *Invest. Radiol.* **2000**, *35* (2), 91–96.
(28) Popovtzer, R.; Agrawal, A.; Kotov, N. A.; Popovtzer, A.; Balter, J.; Carey, T. E.; Kopelman, R. *Nano Lett.* **2008**, *8* (12), 4593–4596.
(29) Weissleder, R.; Lee, A. S.; Fischman, A. J.; Reimer, P.; Shen, T.; Wilkinson, R.; Callahan, R. J.; Brady, T. J. *Radiology* **1991**, *181* (1), 245–249.
(30) Lee, J.-H.; Huh, Y.-M.; Jun, Y.-w.; Seo, J.-w.; Jang, J.-t.; Song, H.-T.; Kim, S.; Cho, E.-J.; Yoon, H.-G.; Suh, J.-S.; Cheon, J. *Nat. Med.* **2006**, *13* (1), 95–99.
(31) Na, H. B.; Lee, J. H.; An, K.; Park, Y. I.; Park, M.; Lee, I. S.; Nam, D.-H.; Kim, S. T.; Kim, S.-H.; Kim, S.-W.; Lim, K.-H.; Kim, K.-S.; Kim, S.-O.; Hyeon, T. *Angew. Chem., Int. Ed.* **2007**, *46* (28), 5397–5401.
(32) Liu, S.; Jia, B.; Qiao, R.; Yang, Z.; Yu, Z.; Liu, Z.; Liu, K.; Shi, J.; Ouyang, H.; Wang, F.; Gao, M. *Mol. Pharmaceutics* **2009**, *6* (4), 1074–1082.
(33) Yang, L.; Mao, H.; Cao, Z.; Wang, Y. A.; Peng, X.; Wang, X.; Sajja, H. K.; Wang, L.; Duan, H.; Ni, C.; Staley, C. A.; Wood, W. C.; Gao, X.; Nie, S. *Gastroenterology* **2009**, *136* (5), 1514–1525.
(34) Park, J.-H.; von Maltzahn, G.; Zhang, L.; Derfus, A. M.; Simberg, D.; Harris, T. J.; Ruoslahti, E.; Bhatia, S. N.; Sailor, M. J. *Small* **2009**, *5* (6), 694–700.
(35) Khemtong, C.; Kessinger, C. W.; Ren, J.; Bey, E. A.; Yang, S.-G.; Guthi, J. S.; Boothman, D. A.; Sherry, A. D.; Gao, J. *Cancer Res.* **2009**, *69* (4), 1651–1658.
(36) Chen, T.-J.; Cheng, T.-H.; Chen, C.-Y.; Hsu, S. C. N.; Cheng, T.-L.; Liu, G.-C.; Wang, Y.-M. *J. Biol. Inorg. Chem.* **2009**, *14* (2), 253–260.
(37) Park, J.-H.; von Maltzahn, G.; Zhang, L.; Schwartz, M. P.; Ruoslahti, E.; Bhatia, S. N.; Sailor, M. J. *Adv. Mater.* **2008**, *20* (9), 1630–1635.
(38) Hultman, K. L.; Raffo, A. J.; Grzenda, A. L.; Harris, P. E.; Brown, T. R.; O'Brien, S. *ACS Nano* **2008**, *2* (3), 477–484.
(39) van Vlerken, L. E.; Vyas, T. K.; Amiji, M. M. *Pharm. Res.* **2007**, *24* (8), 1405–1414.
(40) Howard, M. D.; Jay, M.; Dziubla, T. D.; Lu, X. *J. Biomed. Nanotechnol.* **2008**, *4* (2), 133–148.
(41) Choi, H. S.; Liu, W.; Misra, P.; Tanaka, E.; Zimmer, J. P.; Ipe, B. I.; Bawendi, M. G.; Frangioni, J. V. *Nat. Biotechnol.* **2007**, *25* (10), 1165–1170.
(42) Eck, W.; Craig, G.; Sigdel, A.; Ritter, G.; Old, L. J.; Tang, L.; Brennan, M. F.; Allen, P. J.; Mason, M. D. *ACS Nano* **2008**, *2* (11), 2263–2272.
(43) Herrwerth, S.; Rosendahl, T.; Feng, C.; Fick, J.; Eck, W.; Himmelhaus, M.; Dahint, R.; Grunze, M. *Langmuir* **2003**, *19* (5), 1880–1887.
(44) Nokta, M. A.; Li, X.-D.; Nichols, J.; Mallen, M.; Pou, A.; Asmuth, D.; Pollard, R. B. *AIDS* **2001**, *15* (2), 161–169.
(45) Gupta, R.; Grasruck, M.; Suess, C.; Bartling, S. H.; Schmidt, B.; Stierstorfer, K.; Popescu, S.; Brady, T.; Flohr, T. *Eur. Radiol.* **2006**, *16* (6), 1191–1205.
(46) Owens, D. E.; Peppas, N. A. *Int. J. Pharm.* **2006**, *307* (1), 93–102.
(47) Koo, O. M.; Rubinstein, I.; Onyuksel, H. *Nanomedicine* **2005**, *1* (3), 193–212.
(48) Reddy, L. H. *J. Pharm. Pharmacol.* **2005**, *57* (10), 1231–1242.
(49) van Vlerken, L. E.; Amiji, M. M. *Expert Opin. Drug Delivery* **2006**, *3* (2), 205–216.
(50) Cho, K.; Wang, X.; Nie, S.; Chen, Z.; Shin, D. M. *Clin. Cancer Res.* **2008**, *14* (5), 1310–1316.
(51) Pirollo, K. F.; Chang, E. H. *Trends Biotechnol.* **2008**, *26* (10), 552–558.

DOI: 10.1021/nl101019s | *Nano Lett.* **XXXX,** *xxx,* 000–000